A single-probe-beam double-heterodyne polarimeter-interferometer for plasma Faraday rotation measurements

J. Howard,[1, a)] J. Muir,[1] F. Glass,[1] and N. Hicks[2]
[1)] *Plasma Research Laboratory, The Australian National University, Canberra ACT 0200 Australia*
[2)] *College of Engineering, University of Washington, Seattle WA 98195-2400 USA*

(Dated: 5 March 2012)

This article describes a novel polarimetry configuration that solves a number of technical issues that can complicate the small Faraday rotation angles imparted on a probing laser beam that traverses a magnetized plasma.

I. INTRODUCTION

The rotation of the polarization of a linearly-polarized probing laser beam traversing a magnetized plasma is a useful electron density or internal magnetic field diagnostic[1,2]. The Faraday rotation angle of the electric vector is given by[3]:

$$\psi \approx 2.6 \times 10^{-13} \lambda_0^2 \int_0^L n_\mathrm{e} B_\parallel \mathrm{d}l. \qquad (1)$$

where λ_0 is the laser vacuum wavelength (typically infrared to far-infrared) and $B_\parallel = \boldsymbol{B}.\hat{\boldsymbol{l}}$, where $\boldsymbol{B}$ is the magnetic field, $\hat{\boldsymbol{l}}$ is the unit vector in the laser propagation direction, n_e is the electron density, $\mathrm{d}l$ is a line element and SI units are used. Usually, n_e is determined interferometrically by measuring the accompanying refractive phase shift[3]

$$\varphi = r_\mathrm{e} \lambda_0 \int_0^L n_\mathrm{e} \mathrm{d}l \qquad (2)$$

where r_e is the classical electron radius. Subject to appropriate symmetry assumptions, the parallel magnetic field $B_\parallel$ can be inferred from simultaneous measurements of ψ and φ at a sufficient number of positions across the plasma.

The simplest polarimetric scheme is to measure the intensity of the rotated electric field component through an analyzer oriented to reject the original probe beam polarization[4]. The transmitted component is usually mixed with an independent, frequency offset local oscillator and the amplitude of the resulting beat signal is proportional to ψ. Various other homodyne and heterodyne schemes have also been tried[5–8].

Homodyne schemes require two detectors per spatial channel in order to extract the interferometric and polarimetric phase angles φ and ψ. These systems are difficult to balance in order that beam refraction effects are negligible. Heterodyne schemes require either multiple independent laser sources or mechanical modulators such as rotating gratings or waveplates. Except in the latter case, this requires that the probing sources must also be carefully co-aligned to remove differential refraction effects.

Our approach measures both interferometric and polarimetric information using a chirped microwave source and a single detector per probe beam. Because the system uses only a single radiation source and a single detector per spatial channel, it should be robust against errors caused by refraction within the plasma[7].

This paper is organized as follows. The operating principle of the polarimeter-interferometer and a prototype benchtop system are described in Sec. II with a Jones matrix analysis of the system given in the appendix. Results using the prototype system are presented in Sec. III. The system performs as expected with little crosstalk between the interferometric and polarimetric signals. A multi-channel interferometer/polarimeter based on the principles of the prototype system is now being constructed for Faraday rotation measurements on the helicity injected tokamak HIT-SI[9].

II. OPERATING PRINCIPLE AND EXPERIMENTAL LAYOUT

The layout of the polarimeter-interferometer is shown in Fig. 1. In this scheme, the interferometer is configured as a single-pass system. By replacing two of the interferometer turning mirrors by reflecting waveplates of adjustable path delay (components PR1 and PR2), and using a final polarizer to mix the various wave components, the signal at the detector is sensitive to both the interferometric phase shift the polarization state of the probing radiation emerging from the plasma. The combination of two waveplates of adjustable delay and/or orientation and a final analyzer is a standard approach to recover the Stokes vector describing the state of polarization of light (see for example[10]).

When the source frequency can be swept linearly (or "chirped"), the time delay $\tau = L/c$ between probe and local oscillator beams gives rise a frequency difference between the mixed waves at the detector given by $\omega_i = 2\pi(\partial f/\partial t)\tau$ (see Fig. 1). In practice, a continuous linear chirp is not possible and the frequency must be modulated by a sawtooth wave. By applying a sawtooth control voltage (frequency $\Omega/2\pi$ =1kHz), it is possible to

[a)] john.howard@anu.edu.au

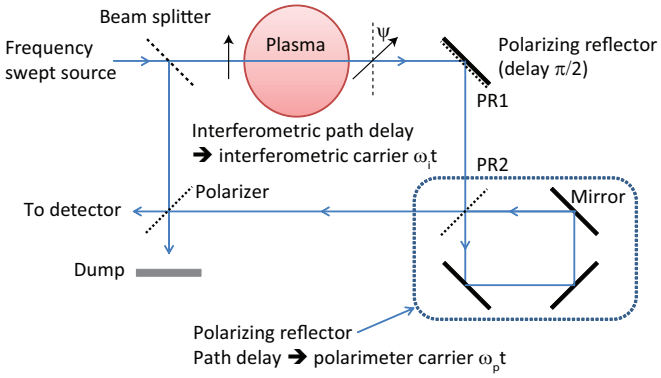

FIG. 1. Schematic layout for the heterodyne polarimeter-interferometer. If each of the polarizing reflectors is replaced by simple mirrors, the system reverts to a standard chirped-source interferometer.

adjust the amplitude of the voltage sweep and the path difference L so that, over one sawtooth period $2\pi/\Omega$, the phase difference at the detector is an integer number of waves $N = (2\pi\tau/\Omega)\partial f/\partial t)$. Ignoring the sawtooth reset discontinuity, this results in an effective heterodyne carrier frequency $\omega_i = N\Omega$.

The birefringent polarizing reflecting elements can be constructed from parallel orthogonal polarizers (or polarizer and backing mirror) whose separation L is also adjustable. By introducing a large path difference, the second waveplate PR2 in Fig. 1 becomes effectively a temporally modulated waveplate of delay $\omega_p t = M\Omega t$ where M is an integer. The combination of independent frequency-offset carriers ω_i and ω_p at harmonics of the sawtooth modulation frequency Ω allows separation of the interferometric and polarimetric phase angles. Using a Jones matrix analysis, it is shown in the appendix, that the signal at the detector output is given by:

$$\begin{aligned} I &= (I_{\rm LO} + I_0/2) + I_0/2\cos(\omega_p t + 2\psi) \\ &+ \sqrt{I_0 I_{\rm LO}}\cos(\omega_i t + \varphi - \psi) \\ &+ \sqrt{I_0 I_{\rm LO}}\cos[(\omega_i + \omega_p)t + \varphi + \psi] \end{aligned} \tag{3}$$

The three distinct heterodyne carriers at $\omega_i = N\Omega$, $\omega_p = M\Omega$ and $\omega_i + \omega_p = (N+M)\Omega$ are enough to recover the interferometric and polarimetric phase angles φ and ψ.

III. RESULTS

The radiation source is a 140 GHz, 25 mW voltage tunable IMPATT diode source (ELVA-1 VCO 140/1)[11]. The quasi-optical interferometer is constructed using polyethylene lenses to control the beam diameter, aluminium mirrors and various free-standing wire grids to manipulate the polarization state. The detector is a horn-coupled ELVA-1 ZBD-6 (zero biased detector), with an optical isolator coupled to the detector to suppress back reflections.

The weak frequency dependence of the source power ($\lesssim 20\%$ variation over the control voltage sweep range) generates harmonic sidebands that couple the various interferometric and polarimetric carriers. However, as the n^{th} harmonic component of a sawtooth wave has amplitude proportional to $1/n$, the crosstalk due to the power non-linearity can be largely suppressed by separating the carriers by more than one harmonic of the sawtooth modulation frequency. In our case, the path lengths and drive voltage were adjusted to give $N = M = 2$ so that the carrier frequencies correspond to the 2^{nd}, 4^{th} and 6^{th} harmonics of the fundamental sawtooth frequency. In practice, this was achieved using an interferometer arm path length difference of 600cm (to generate ω_i) and a delay plate path length difference of 300cm (ω_p). Figure 2 shows the multiple-harmonic detector waveform (solid) and the sawtooth control voltage for two periods of the sawtooth wave. The associated frequency spectrum shows the primary carrier waves at 2, 4 and 6 kHz, and the nonlinearly generated contaminating sidebands at a level 15-20 dB lower.

In order to test the polarimeter performance, a rotatable wire grid polarizer was interposed in the nominal plasma arm to set the polarization angle ψ. Because of its large aperture (100 mm) the polarizer was rotated by mounting it in a circular ring that could be driven by a rigid bar connected to a translation stage, such that 1mm of displacement corresponded approximately 1.1° of polarizer rotation. Figure 3 (top) shows that the measured polarisation angle obtained by ramping up and down the polarizer angle in steps of 1° across an angle range of 10°. The test angle is accurately recovered by the system using the 4kHz and 6kHz carriers, and the rms angle noise for a 10ms integration period is 0.1°. There is some evidence of mechanical backlash in the rotation mechanism when the direction of rotation is reversed. As seen in Fig. 3 (bottom), the coupling between the polarimetric and interferometric angles is small.

IV. CONCLUSION

We have demonstrated a new type of millimeter-wave interferometer/polarimeter that requires a single source and a single detector for each spatial probing beam. A modulated waveplate produced using a chirped microwave source, is used to discriminate between the interferometric and polarimetric angles. A system based on this principle is now being constructed for measurements on the HIT-SI tokamak.

V. APPENDIX

The modified polarization state of a linearly polarized probing beam can be represented by the complex vector

$$\boldsymbol{E} = \begin{pmatrix} \cos\eta \\ \sin\eta \exp j\phi \end{pmatrix} \tag{4}$$

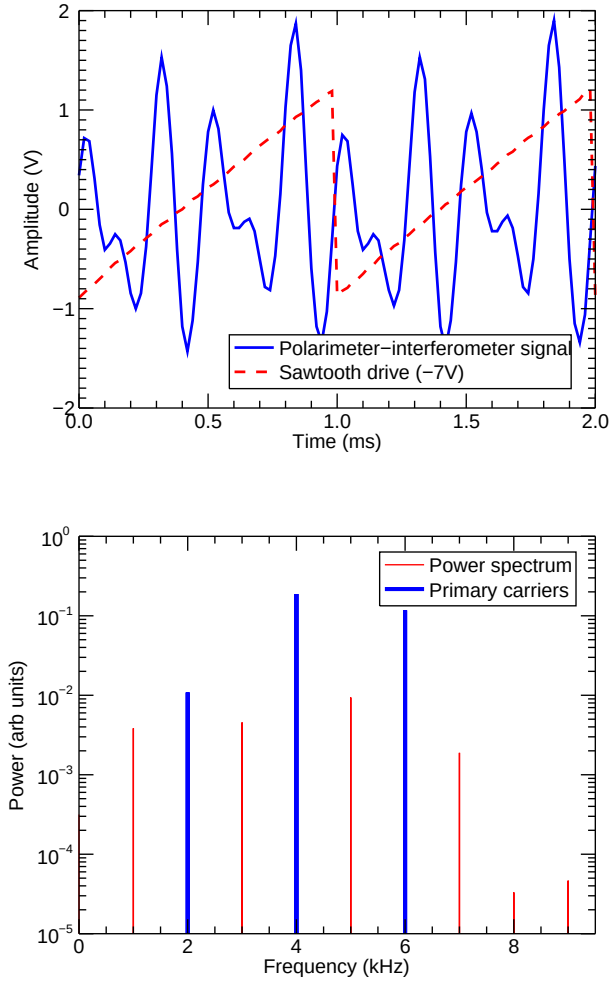

FIG. 2. Top: the sawtooth control signal applied to the frequency swept source (dashed) and the resulting polar-interferometric carrier signal. Bottom: the computed carrier signal power spectrum. The primary polarimetric and interferometric carriers are indicated by the bold traces. Note that the sideband power decreases rapidly away from the principal carriers - see harmonics 7, 8 and 9

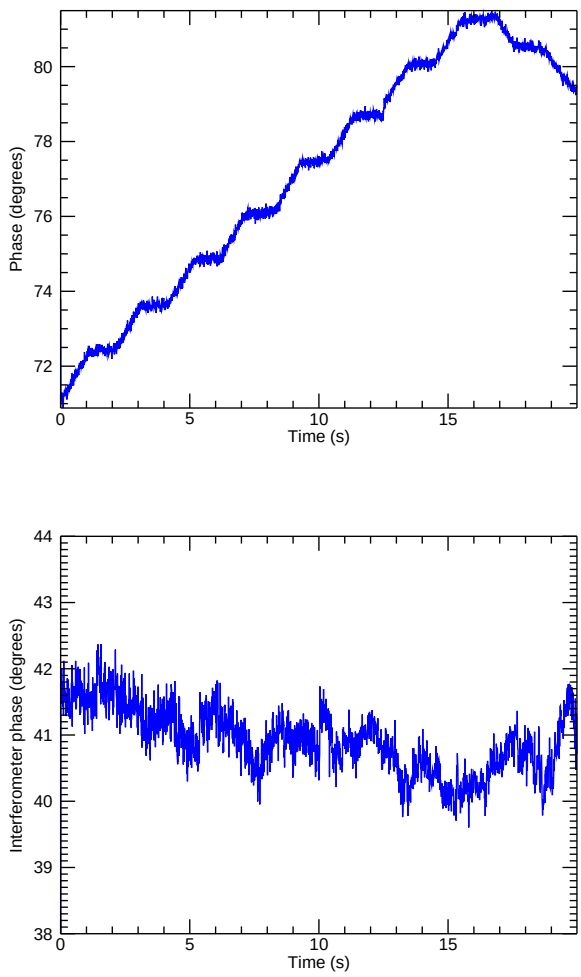

FIG. 3. Top: The observed change in polarization angle as the test polarizer is rotated in approximately 1 degree steps and Bottom: the associated interferometric angle (with an arbitrary DC offset). The traces were smoothed using a boxcar filter of width 10 ms. The coupling between the interferometric and polarization angles is small.

where $\tan\eta = \mid E_y \mid / \mid E_x \mid$ and ϕ is the phase angle between the x and y components of the wave and the time dependence is ignored. The parameters η and ϕ are related to the Faraday rotation ψ of the vibrational ellipse and the ellipticity χ by

$$\tan 2\psi = \tan 2\eta \cos\phi$$
$$\sin 2\chi = \sin 2\eta \sin\phi.$$

The plasma birefringence (Cotton-Mouton effect) is often negligible. It is thus later convenient to ignore this effect, allowing us to set $\phi = 0$ and identify $\eta = \psi$.

The first element of the polarimeter is a retarding optic (reflecting or transmitting) aligned so that the initial electric vector is parallel to one of the characteristic axes. We write its Jones matrix as

$$\boldsymbol{R}_0(\delta_1) = \begin{pmatrix} 1 & 0 \\ 0 & \exp(-2j\delta_1) \end{pmatrix}. \quad (5)$$

with $\delta_1 = \pi/4$ in the case of a quarter wave delay. This is followed by a second delay component oriented at 45° to the first and having Jones matrix

$$\boldsymbol{R}_{45}(\delta_2) = \begin{pmatrix} \cos\delta_2 & j\sin\delta_2 \\ j\sin\delta_2 & \cos\delta_2 \end{pmatrix}. \quad (6)$$

The final component is an ideal analyzer (in our case, a free-standing wire grid polarizer) whose matrix in trans-

mission is

$$\boldsymbol{P}_{\alpha}^{T} = \begin{pmatrix} \sin^2\alpha & -\sin\alpha\cos\alpha \\ -\sin\alpha\cos\alpha & \cos^2\alpha \end{pmatrix} \tag{7}$$

and in reflection $\boldsymbol{P}_{\alpha}^{R} = -\boldsymbol{P}_{\alpha-\pi/2}^{T}$ where α is the polarizer wire orientation. For this polarimeter, the analyzer is oriented at $\alpha = 90°$.

For an initial quarter wave delay followed by a general delay δ, the electric field of the wave transmitted by the final analyzer is given by

$$\boldsymbol{E}_{\mathrm{T}} = \boldsymbol{P}_{90}^{T}\boldsymbol{R}_{45}(\delta)\boldsymbol{R}_{0}(\pi/4)\boldsymbol{E} \tag{8}$$

This can be easily evaluated, leading to complex scalar electric field component

$$\begin{aligned} u_{\mathrm{T}} = \frac{\sqrt{I_0}}{2}\big[&(1+\exp 2j\delta)\cos\eta \\ &- j(1-\exp 2j\delta)\sin\eta\exp j\phi)\big] \end{aligned} \tag{9}$$

where I_0 is the incident laser beam intensity.

In order to encode the polarimetric information it is convenient to inject a local oscillator beam which we write as

$$u_{\mathrm{LO}} = \sqrt{I_{\mathrm{LO}}}\exp\left[-j(\omega_i t + \varphi)\right] \tag{10}$$

where ω_i is the interferometric carrier frequency difference between the LO beam and the probe, φ is the plasma produced interferometric phase shift and I_{LO} is the local oscillator intensity. The combined intensity on a square law detector is given by $I = \mid u_{\mathrm{T}} + u_{\mathrm{LO}} \mid^2$. In the interests of simplicity we assume the plasma linear birefringence is negligible and take $\phi = 0$ and $\psi \equiv \eta$. The intensity at the detector can then be written

$$\begin{aligned} I = I_{\mathrm{LO}} &+ I_0/2\big[1+\cos(2\psi+2\delta)\big] \\ &+ \sqrt{I_0 I_{\mathrm{LO}}}\cos(\omega_i t + \varphi - \psi) \\ &+ \sqrt{I_0 I_{\mathrm{LO}}}\cos(\omega_i t + \varphi + \psi + 2\delta) \end{aligned} \tag{11}$$

For a frequency swept source, it is possible to construct the final waveplate delay such that $2\delta = \omega_p t$ where $\omega_p t$ is the polarimetric carrier frequency. In practice, the optical path lengths giving rise to both ω_i and ω_p are chosen such that the carrier frequencies are integer multiples of the frequency $\Omega/2\pi$ of the control sawtooth wave applied to the microwave source. The final result indicates that the detector will see carrier signals at three distinct frequencies ω_p, ω_i and $\omega_i + \omega_p$ carrying independent phase modulations 2ψ, $\varphi - \psi$ and $\varphi + \psi$ respectively. It is straightforward to demodulate the carrier signals to recover the Faraday angle ψ and the interferometer phase shift φ. The scheme proposed here is reminiscent of, but much simpler than the multiple laser-beam scheme proposed elsewhere[8].

ACKNOWLEDGEMENTS

The authors would like to acknowledge the expert technical assistance provided by Mark Gwynneth.

REFERENCES

[1] F. DeMarco and S. E. Segre, Plasma Phys. **14**, 245 (1972).
[2] S. E. Segre, Plasma Phys. **20**, 295 (1978).
[3] D. Véron, in *Infrared and Millimeter Waves*, edited by K. Button (Academic Press, New York, 1979), Vol. 2, pp. 69–135.
[4] H. Soltwisch, Infrared Phys. **21**, 287 (1981).
[5] G. Dodel and W. Kunz, Infrared Phys. **18**, 773 (1978).
[6] R. Erickson, P. Forman, and F. Jahoda, IEEE Trans. Plasma Sci. **AP-17**, 275 (1984).
[7] B. W. Rice, Rev. Sci. Instrum. **63**, 5002 (1992).
[8] J. H. Rommers and J. Howard, Plasma Phys. Control. Fusion **38**, 1805 (1996).
[9] T. Jarboe *et al.*, Nuclear Fusion **51**, 063029 (2011).
[10] J. Howard, C. Michael, F. Glass, and A. Danielsson, Plasma Phys. Control Fusion **45**, 1143 (2003).
[11] ELVA-1, 46 Robezu, LV-1004, Riga, Latvia.